Ceramics International **21** (1995) 445–449

Structural Changes of Micropores in Carbons by Chemical Vapor Infiltration of Carbon

Yoshihito Shigeno,[a] James W. Evans,[b] & Itsumei Yoh[c]

[a]Division of International Cultural Studies, Graduate School of Tohoku University, Sendai, 980–77, Japan
[b]Dept of Materials Science and Mineral Engineering, University of California, Berkeley, CA, 947320, USA
[c]Coulter Japan Scientific Instruments Company, Ltd, 6-7-5 Higashi Kasai, Tokyo 134, Japan

(Received 11 November 1994; accepted 17 January 1995)

Abstract: Chemical vapor infiltration is now being used to produce advanced materials for aerospace applications. It is also applicable to carbons to enhance the resistance against oxidation. In the present study, methane pyrolysis was conducted for several kinds of carbons such as electrode-grade graphite, electrode-grade carbon, coke and activated charcoal. The structural change of micropores (radius <10 nm) accompanying infiltration and oxidation was investigated because oxidation is considered mainly to occur in such small pores due to their large specific surface area. The change of macropores measured by mercury porosimeter is also shown for comparison with that of fine pores. Pore-size distribution measured by the BET method have shown that the filling mode depends on the pore structure of carbons.

1 INTRODUCTION

To increase the resistance to oxidation with CO_2 ($C + CO_2 = 2CO$), five kinds of carbons such as activated charcoal (A.C.), formed coke (F-coke), metallurgical coke (M-coke), electrode-grade graphite (E.G.) and electrode-grade carbon (E.C.) were infiltrated by carbon produced through methane pyrolysis ($CH_4 = 2H_2 + C$). The pore within carbons was filled by carbon, therefore, the treated carbon increased the resistance against oxidation. The direct application of this technology is upgrading of coke so as to have higher CSR (Coke Strength after CO_2 Reaction). The modified coke showed an improvement of mechanical strength after oxidation as well.[1–3]

We have so far paid attention to the phenomena occurring in macropore (r >10 nm)[1,4] the range of which is adequate for measurement by a mercury porosimeter. However, the pores smaller than about 10 nm in radius cannot be measured precisely by this method. The drastic change of surface area of pore accompanying infiltration or oxidation had been expected because the magnitude of the area is getting extremely large with decreasing pore size.

Therefore, in the present study, the changes of pore-size distribution from about 1 to 50 nm were measured by use of BET. The change of macropores of A.C. is also shown for discussion of the effect of infiltration.

2 EXPERIMENT

The apparatus is the same as that reported previously,[1,4] the formed coke, E.G. and E.C. were cut into slabs (25·4 mm in height, 25·4 mm in width and 3 mm in thickness). They were suspended in the uniform temperature zone (±5K) of the furnace with a stainless steel wire. Figure 1 shows the case in which four plates are being suspended for infiltration. The activated charcoal, metallurgical coke were small grains the diameter of which was about 4 mm. Several grains were put into the basket made of stainless steel wire and suspended by the stainless wire in the same manner as shown in

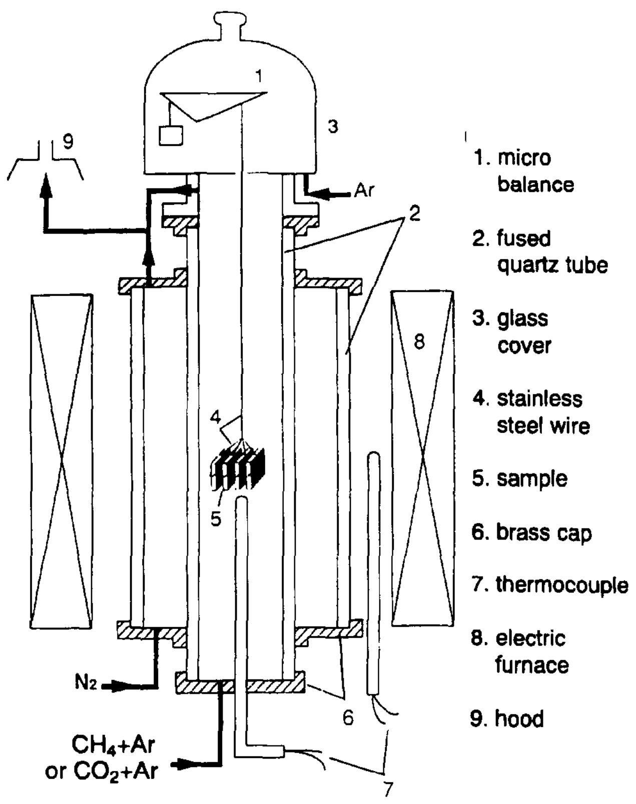

Fig. 1. Schematic diagram of experimental apparatus.

Fig. 1. The infiltration and oxidation rates were determined by monitoring the weight continuously.

The reaction gas for infiltration was a mixture of methane (24%) and argon which was introduced from the bottom of the reaction tube. The flow rate of the gas mixture was 9·7 $\times 10^{-6}$ m^{-3} s^{-1} (0·58 litre min^{-1}).

Oxidation followed the infiltration experiment with changes in only a few experimental conditions; the reaction gas was a mixture of Ar and CO_2 (10%), the gas flow rate was 5×10^{-5} m^{-3} s^{-1} (3 litre min^{-1}), the experimental temperature was 1223 K.

3 EXPERIMENTAL RESULTS

3.1 Weight increase with time due to infiltration

In Fig. 2, the fractional weight increase during infiltration for A. C. and M-coke is shown. The curves in this figure show the monotonous increase with time and the slightly different mode of increase among the samples. Especially, the initial rate which was very large for the activated charcoal.

3.2 Comparison of oxidation rate between original and infiltrated samples

Figure 3 shows the comparison of the oxidation rates of A.C. for original and infiltrated ones. The oxidation rate (the slope of fractional weight decrease with time) decreased by about 50% for the infiltrated sample from the original one. This is the typical example showing the upgrading of the resistance to oxidation by infiltration. For other carbons, the mode of the decrease in oxidation rate is similar to A.C. The ratio of the oxidation rate of infiltrated sample to the original one for other carbons is compared in Fig. 10, in which

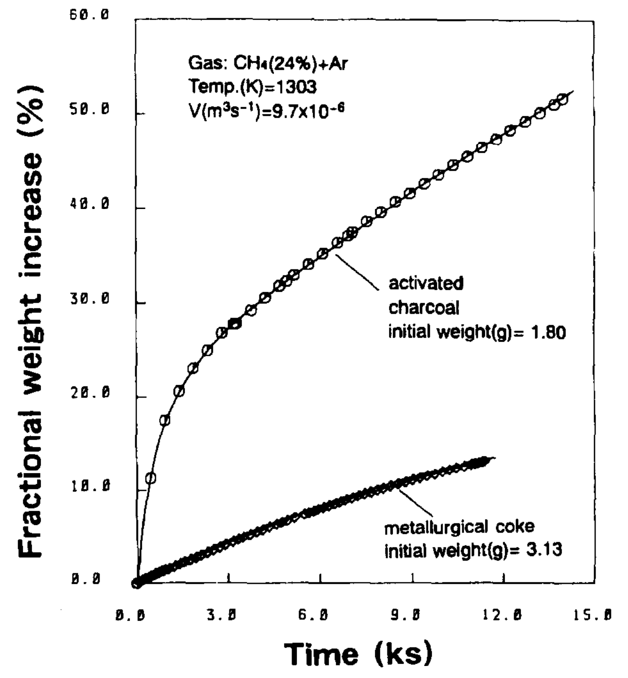

Fig. 2. Fractional weight increase with time for metallurgical coke and activated charcoal.

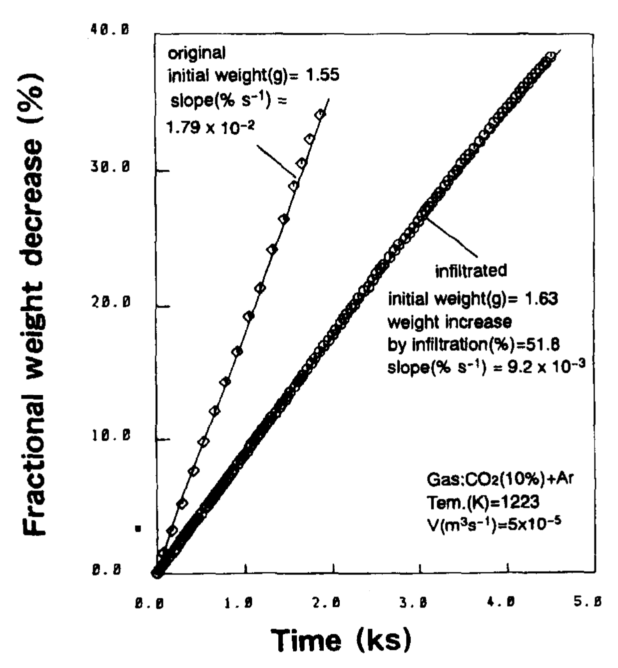

Fig. 3. Comparison of oxidation rates between original and infiltrated activated charcoal.

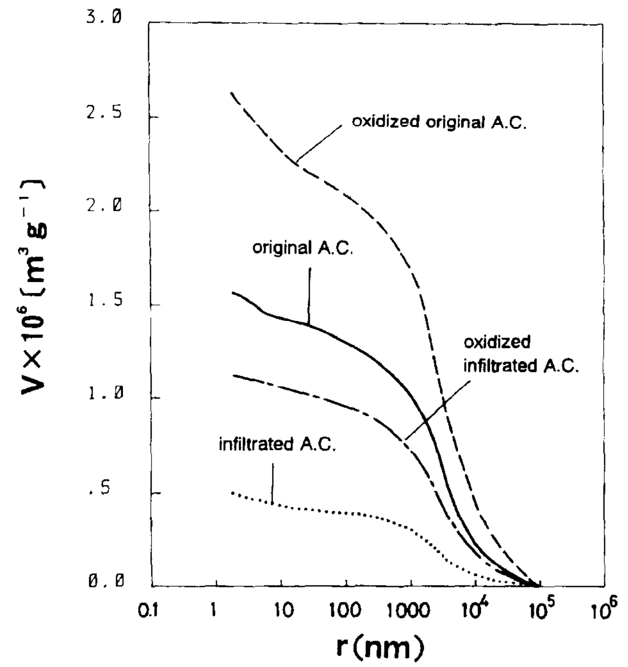

Fig. 4. Changes in cumulative pore volume of original, infiltrated and oxidised (original and infiltrated) activated charcoal (A.C.).

the value is 45% for E.C., 66% for metallurgical coke and about 80% for formed coke and E.G.

3.3 Measurement of pore-size distribution by mercury porosimeter

Figure 4 shows the changes of cumulative pore volume of A.C. corresponding to the following treatment: (i) original, (ii) oxidized, (iii) infiltrated, and (iv) infiltrated and then oxidized. This is the typical example of the change of pore-size distribution accompanying infiltration and oxidation.

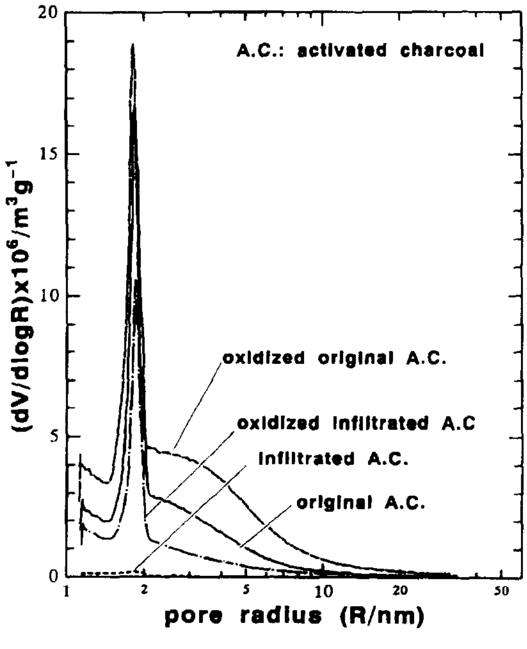

Fig. 5. Change in pore-size distribution of fine pore of original, infiltrated and oxidised (original and infiltrated) activated charcoal.

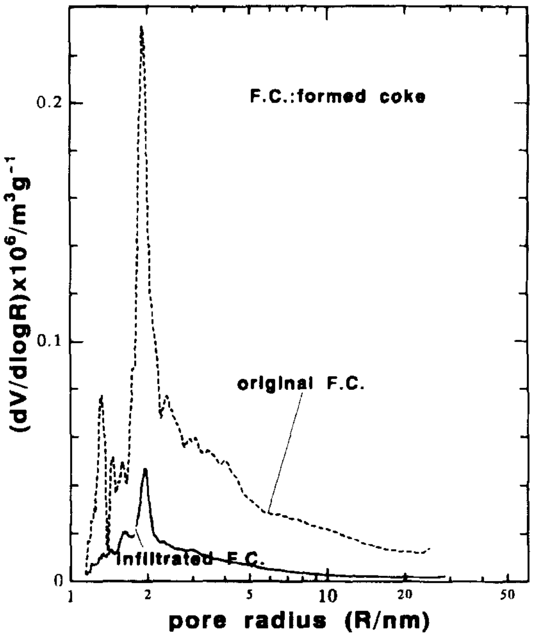

Fig. 6. Change in pore-size distribution of fine pore of original and infiltrated formed coke.

3.4 Measurement of pore-size distribution by BET

The pore characteristic change under 50 nm was measured by the BET method. The result is shown in Figs 5–9. These figures show the pore volume distribution with pore radius for the A.C. (Fig. 5), F-coke (Fig. 6), M-coke (Fig. 7), E.C (Fig. 8), and E.G. (Fig. 9), respectively. The specific volume and the specific surface area after infiltration and

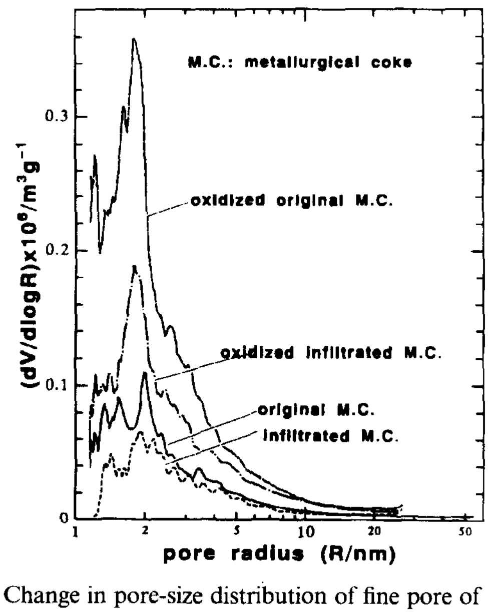

Fig. 7. Change in pore-size distribution of fine pore of original, infiltrated and oxidised (original and infiltrated) metallurgical coke.

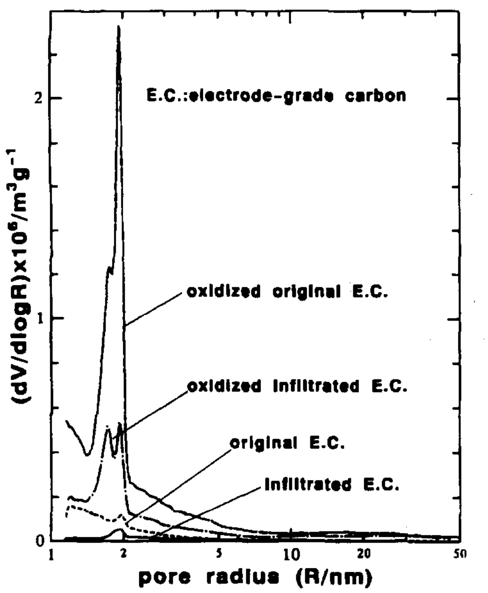

Fig. 8. Change in pore-size distribution of fine pore of original, infiltrated and oxidised (original and infiltrated) electrode-grade carbon.

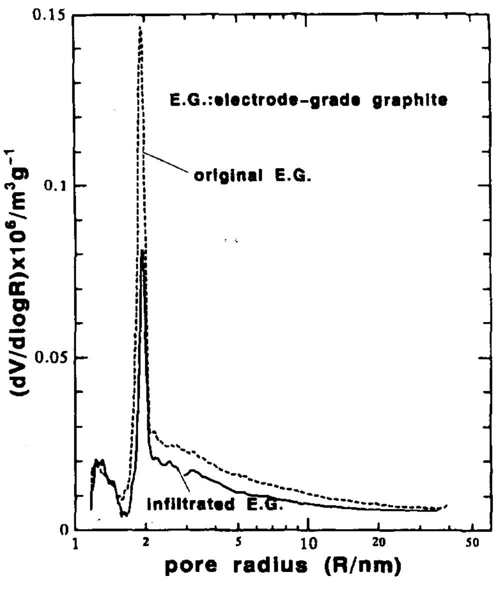

Fig. 9. Change in pore-size distribution of fine pore of original and infiltrated electrode-grade graphite.

oxidation measured by BET are summarized in Table 1. The ratio of these values of the infiltrated carbon to the original one is also graphically represented in Fig. 10.

In the case of A.C., the volume of infiltrated sample decreased to about 3% of the original value. The volume of the formed coke decreased to 19%. However, the other carbons did not represent such a large decrease: 67% for E.G., 76% for metallurgical coke, 50% for E.C.

Oxidation enlarges the pore size both for the original and infiltrated samples. This change is measured for A.C., M-coke and E.C. and is shown in Figs 5, 7 and 8, respectively. In each case, the increase in pore volume by oxidation is larger for the untreated original carbons than for the infiltrated ones. Figures 5, 7 and 8 show that oxidation proceeds in the entire range of pore radius ($1 < r < 30$ nm) and increase in volume is very large near 2 nm in radius; in the range above 10 nm, the change in pore volume is relatively small for all the samples.

4 DISCUSSION

4.1 Infiltration and oxidation rates

The pyrolytic carbon accumulates on the surface of pores. Accumulation is considered to occur in both macro and micropore. However, at the beginning of infiltration, its rate is larger for the

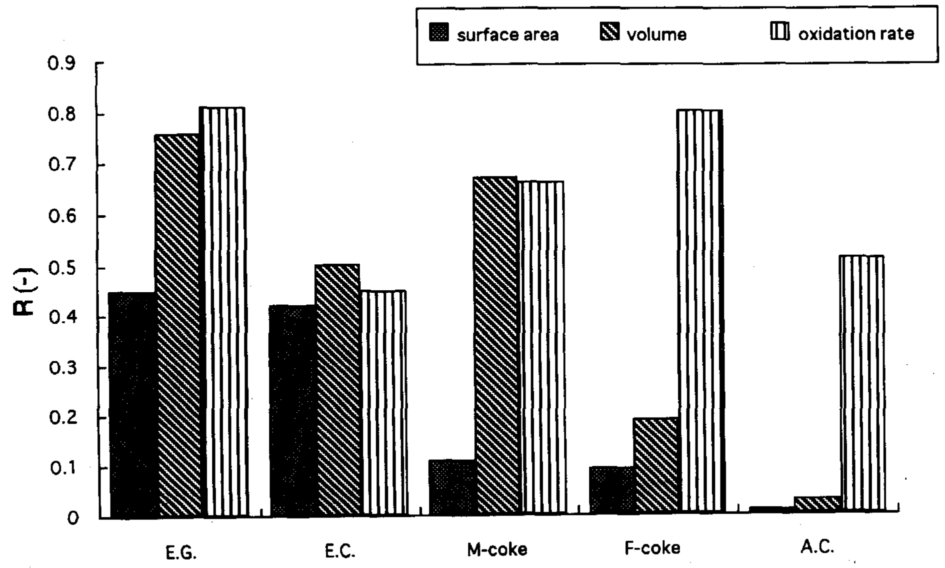

Fig. 10. Decrease in surface area, volume and oxidation rate due to infiltration. The ordinate (R) is the ratio of respective value of infiltrated carbon to that of original one.

Table 1. Surface area and pore volume measured by BET for various carbons

	BET surface area (m^3/g)	Total pore volume (>1 nm) (mm^3/g)
Electrode-grade graphite		
original	1·4952	6·15
infiltrated	0·67	4·65
Formed coke		
original	2·3904	10·28
infiltrated	0·2162	1·97
Activated charcoal		
original	697·11	239·4
infiltrated	6·0794	6·92
oxidized original	911·92	437·4
oxidized infiltrated	182·00	123·9
Electrode-grade carbon		
original	0·5203	6·49
infiltrated	0·2176	3·26
oxidized original	46·302	40·14
oxidized infiltrated	7·982	23·16
Metallurgical coke		
original	1·296	6·78
infiltrated	0·1446	4·53
oxidized original	21·243	14·32
oxidized infiltrated	8·1057	9·53

former pore because of easier access of methane to this pore. As infiltration proceeds, the volume of macropore decreases rapidly. This causes the decrease in the infiltration rate. On the other hand, the oxidation rate is almost constant in spite of the increase of pore size. This constant oxidation rate is often found for other untreated carbons but the reason is not yet obvious.

4.2 Structural changes of the pore measured by mercury porosimeter

The pore structures of A.C. show the distinctive bimodal mode as seen with the curve of the original one. The slope ($-dV/d\log r$) means the pore distribution and the steep slopes are observed in the vicinity of 1000 nm and 3 nm, i.e. at these ranges, the major volume of the pores is distributed. The infiltrated A.C. exhibits a decrease in slope over the entire range. Conversely, during oxidation, the pore of the original A.C. was enlarged over all the range, especially at 3 and 1000 nm. However, for the infiltrated A.C., the pore under about 300 nm was not enlarged. This fact implies the importance of considering the micropore.

4.3 Structural change of the pore measured by BET

The micropore is the interstice existing between the parallel groups of graphite crystal lattice. The space characteristic of carbon of about 2 nm in radius was observed for all the samples. These results show that methane intrudes into these small interstices and infiltration occurs. Additionally, during oxidation, carbon dioxide intrudes and oxidizes the deposited carbon. The infiltration mode is different depending on the pore structure.

Figure 10 implies that the surface area and the volume of A.C. decreased extensively by infiltration as already described in Section 3.4, thereby, the oxidation rate was depressed. Actually, increase in both values accompanying oxidation was less for infiltrated A.C. than for the original one as shown in Table 1. On the other hand, the cumulative volume of the macropore decreased to only 1/3 of the original A.C. as shown in Fig. 4. These facts demonstrate the importance of infiltration within micropores.

Concerning the carbons other than A.C., Fig. 10 describes that the decrease ratio of pore size was not remarkable. This is because the total volume of micropore of A.C. is larger by more than 100 times than the other carbons as shown in Table 1. Comparison of the ratio of decrease in oxidation rate for E.C. and E.G. in Fig. 10 revealed that the decrease in oxidation rate is larger for E.C. than for E.G. despite the ratio of decrease in surface area being almost the same. The situation is the same for metallurgical coke and formed coke. This is caused by the different filling mode shown in Figs 6, 7, 8 and 9. However, the quantitative discussion of the decrease in oxidation rate based on the pore size distribution or other factors, e.g. crystal structure, is beyond the present report.

5 CONCLUSION

Several kinds of carbon were infiltrated by pyrolytic carbon from methane. The change of pore-size distribution of micropore within these carbons was measured by use of BET. It was found that the infiltration mode depends on the pore structures and the resulting filling mode determines the properties of modified carbons such as upgrading the resistance against oxidation.

REFERENCES

1. SHIGENO, Y. & EVANS, J. W., *Met. Trans.*, **23B** (1992) 429.
2. VANDEZANDE, J. A., *Paper presented at the 16th Biennial Conf. on Carbon.* American Carbon Society, San Diego, CA, 1983, p. 611.
3. UEBO, K., INOUE, K. & NISHIOKA, K., *Paper presented at the 125th ISIJ Annu. Meet.* ISIJ Yokohama, Japan, 1993, p. S51.
4. SHIGENO, Y. & EVANS, J. W., *ISIJ Int.*, **7** (1993) 721.
5. LUCUS, P. & MARCHAND, A., *Carbon*, **28** (1990) 207.